Pure Appl. Chem., Vol. 74, No. 9, pp. 1739–1749, 2002.

Substrate temperature dependence of electrical conduction in nanocrystalline CdTe:TiO_2 sputtered films*

S. N. Sharma[1,‡], S. M. Shivaprasad[2], Sandeep Kohli[3], and A. C. Rastogi[1]

[1]Materials Division, [2]Surface Physics Group, National Physical Laboratory, Dr. K. S. Krishnan Marg, New Delhi 110012, India; [3]Department of Chemistry, Colorado State University, Fort Collins, CO 80523, USA

Abstract: TiO_2 thin films with high volume fraction (~50–70 %) of CdTe nanoparticles were prepared by radio frequency (rf) magnetron sputtering from a composite TiO_2:CdTe target. With increase in substrate temperature T_s from room temperature (RT ~ 300 K) to 373 K, a transition from an ordered structure exhibiting metallic-type conduction to a disordered structure exhibiting nonmetallic-type conduction was observed for annealed nanocrystalline CdTe:TiO_2 films. The annealed RT-deposited films showed a large coalescence of distinct islands (size ~0.3–0.7 μm) mainly of Cd and CdTe, and as result, a 3D network was realized. For metallic regime films, electrical conduction is essentially due to electrical percolation through Cd/CdTe crystallites embedded in an amorphous TiO_2 matrix. However, the annealed high T_s films consisted of noncoalescent, small islands (size ~0.15–0.3 μm) of Cd and CdTe embedded in amorphous TiO_2 matrix. Here, the conduction is essentially by hopping mechanism via thermally activated tunneling.

INTRODUCTION

Nanocomposite films of semiconductors and insulators have been the subject of intensive studies from both fundamental, experimental, and applied interests [1]. CdS, CdSe, and CdTe are among the most studied cases [2]. CdTe, owing to its large exciton Bohr diameter (15 nm), is a strong contender for the future low-dimensional optoelectronic devices [3]. Although the optical properties of nanocomposite films have been studied intensively, the electrical transport properties of these films are not fully understood. Therefore, it is imperative to understand the electron transport process in these low-dimensional structures having different sets of grain size and inter-grain size. Thus, by varying the substrate temperature (T_s) during deposition, a series of films with different grain sizes and inter-grain separations could be obtained. Among the various physical vapor deposition (PVD) techniques for the preparation of CdTe nanocrystalline composites in TiO_2 matrix, rf sputtering has been the most versatile and proven one, since it enables the controlled distribution of nanoparticle size and volume over a wide range [4]. Moreover, using rf magnetron sputtering, the processing at relatively low temperatures can avoid the possible reaction between the matrix and the semiconductor nanoparticles [4].

The present work reports detailed electrical studies of 0.5 μm rf magnetron co-sputtered nanocrystalline CdTe:TiO_2 composite thin films deposited at low and high T_s (RT and 373 K), respec-

Pure Appl. Chem.* **74, 1489–1783 (2002). An issue of reviews and research papers based on lectures presented at the 2nd IUPAC Workshop on Advanced Materials (WAM II), Bangalore, India, 13–16 February 2002, on the theme of nanostructured advanced materials.

‡Corresponding author: Present address: Radiation Laboratory, University of Notre Dame, Notre Dame, Indiana, IN 46556, USA; Tel.: 574-631-5407; Fax: 574-631-8068; E-mail: sharma@hertz.rad.nd.edu

tively. It was observed that the substrate temperature had a profound effect on the electrical conduction properties of nanocrystalline CdTe:TiO_2 composite thin films. The effect of thermal treatment was also envisaged in order to have a further insight on the electrical transport properties of CdTe:TiO_2 composite thin films. X-ray photoelectron spectroscopic studies were performed on as-deposited and thermally treated nanocrystalline CdTe:TiO_2 composite thin films in order to elucidate the nature of the changes in composition in these films, and the results were correlated with the electrical properties of these films.

EXPERIMENTAL

The CdTe nanocrystallites embedded in TiO_2 matrix were prepared by rf magnetron sputtering from a composite target. The target consisted of a TiO_2-sintered disc of 2 inches diameter having a CdTe pellet of 10 mm diameter placed at its center. The volume fraction of CdTe in CdTe:TiO_2 composite thin films was systematically increased by increasing the number of CdTe pellets on the target. TiO_2 and CdTe were co-sputtered with an rf power of 240–260 watts in the presence of Ar gas at 0.02 mbar. The deposition of CdTe:TiO_2 composite thin films of thickness ~0.5 μm was done on glass substrates held at 300 K (RT) and 373 K. The thicknesses of the films were measured using quartz crystal thickness monitor. The thermal treatment of CdTe:TiO_2 films was carried out for an hour in the temperature range 250–300 °C in a vacuum of 10^{-3} torr. The volume fraction of CdTe (V_f) in the films was determined by X-ray photoelectron spectroscopy (XPS) studies. The XPS measurements were performed in an ultra-high vacuum (UHV) chamber (PHI 1257) with a base pressure of 4×10^{-10} torr. The sample is mounted on a molybdenum holder mounted on a high-precision manipulator with x, y, z, and θ degrees of freedom. X-ray photoelectron spectrometer consists of MgK_α (1253.6 eV) source and a high-resolution spherical capacitor electron energy analyzer (279.4 mm diameter with 25 meV resolution). Scanning electron microscopic studies were carried out on as-deposited and thermally treated CdTe:TiO_2 composite thin films in order to understand their surface morphology. The interplanar distance of the films was determined by X-ray diffraction (XRD) studies using a Siemens D500 diffractometer (CuK_α line). DC conductivity measurements in the range ($170 < T < 520$ K) were carried out in a vacuum of 10^{-3} torr. The resistivity in coplanar geometry, using gold film contacts, was measured using a Keithley (617) electrometer.

RESULTS AND DISCUSSION

XPS studies

The stoichiometric and bonding changes in nanocrystalline CdTe:TiO_2 composite thin films prepared at low and high T_s (RT and 373 K) with varied volume fraction of CdTe nanoparticles ($V_f \sim$ 50–70 %) before and after thermal treatment are monitored by core-level XPS studies, and the results are summarized in Table 1. XPS spectra were obtained after argon sputtering (i.e., only the bulk of the film was considered, and surface-related changes were avoided). All data were corrected for electrostatic charging using the XPS lines of C 1s as internal reference energy. As shown in Fig. 1a (curve a), for low T_s (RT) film ($V_f \sim$ 65 %), the presence of Cd $3d_{5/2}$ peak at 405.3 eV indicates that Cd exists either in metallic form (i.e., unreacted Cd) or in CdTe form [5]. Similarly, from Fig. 1b (curve a), the Te peak position at 572.8 eV represents Te either in free state (i.e., unreacted or bonded with Cd) that is, in CdTe form [5]. For as-deposited high T_s (373 K) film, the presence of Cd $3d_{5/2}$ peak at 404.8 eV indicates that Cd still exists either in metallic form or in CdTe form (Fig. 2a, curve a). From Fig. 2b (curve a), the Te $3d_{5/2}$ peak at 572.0 eV indicates the presence of CdTe band. As shown in Table 1, both low (RT) and high (373 K) T_s deposited films are found to be cadmium-rich, which may be due to the higher vapor pressure of Cd as compared to Te during film formation. Upon thermal treatment for low T_s (RT) film ($V_f \sim$ 65 %), the peak position of Cd $3d_{5/2}$ at 404.9 eV and Te $3d_{5/2}$ at 572.3 eV (Figs. 1a and 1b,

Table 1 Determination of sample composition (atomic %) and XPS peak positions for nanocrystalline CdTe:TiO_2 films (AD: as-deposited; AT: after-thermal treatment).

System	T_s (K)	XPS peak positions (eV)		Sample composition from XPS analysis (atomic %)		Cd/Te	
		AD	AT	AD	AT	AD	AT
CdTe:TiO_2 (3 pellets of CdTe)	300	Cd $3d_{5/2}$: 405.3 Te 3 $d_{5/2}$: 572.8 O 1s: 530.3 Ti $2p_{3/2}$: 458.4	Cd $3d_{5/2}$: 404.9 Te $3d_{5/2}$: 572.3 and 575.5 O 1s: 531.3 Ti $2p_{3/2}$: ——-	Cd: 44.0 Te: 20.7 O: 29.1 Ti: 6.1	Cd: 50 Te: 7.4 O: 42.7 Ti : ——-	2.12	6.75
CdTe:TiO_2 (3 pellets of CdTe)	373	Cd $3d_{5/2}$: 404.8 Te $3d_{5/2}$: 572.0 O 1s: 529.8 Ti $2p_{3/2}$: 457.7	Cd $3d_{5/2}$: 405.3 Te $3d_{5/2}$: 577.3 and 580.5 O 1s: 536.0 Ti 2p: ——-	Cd: 41.0 Te: 30.0 O: 25.0 Ti: 3.04	Cd: 43.0 Te: 7.0 O: 50.0 Ti: ——-	1.36	6.14

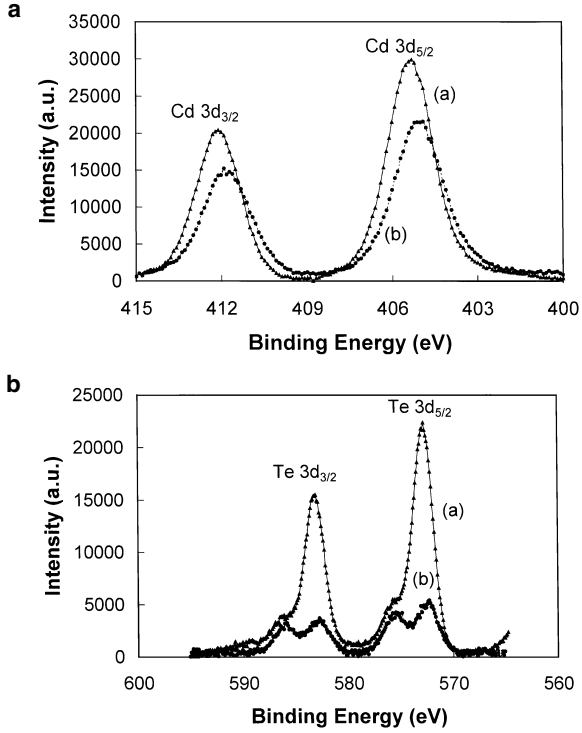

Fig. 1 XPS spectra of CdTe:TiO_2 thin film with $V_f \sim 65$ %, $T_s = 300$ K for (a) Cd $3d_{5/2}$ and Cd $3d_{3/2}$ levels; (a) as-deposited film; (b) the corresponding thermally treated film. (b) for Te $3d_{5/2}$ and Te $3d_{3/2}$ levels; (a) as-deposited film; (b) the corresponding thermally treated film.

curves b) is indicative of the fact that Cd and Te are still bonded to each other [5]. However, the corresponding peak positions for thermally treated high T_s (373 K) films are 405.3 and 577.3 eV (Figs. 2a and 2b, curves b) which indicates the possible formation of $Cd(OH)_2$ and TeO_3, respectively [6]. Although for both low and high T_s deposited films, no evidence of the splitting of the Cd 3d doublet was found upon thermal treatment, however, the Te 3d binding energies deviate considerably. As shown

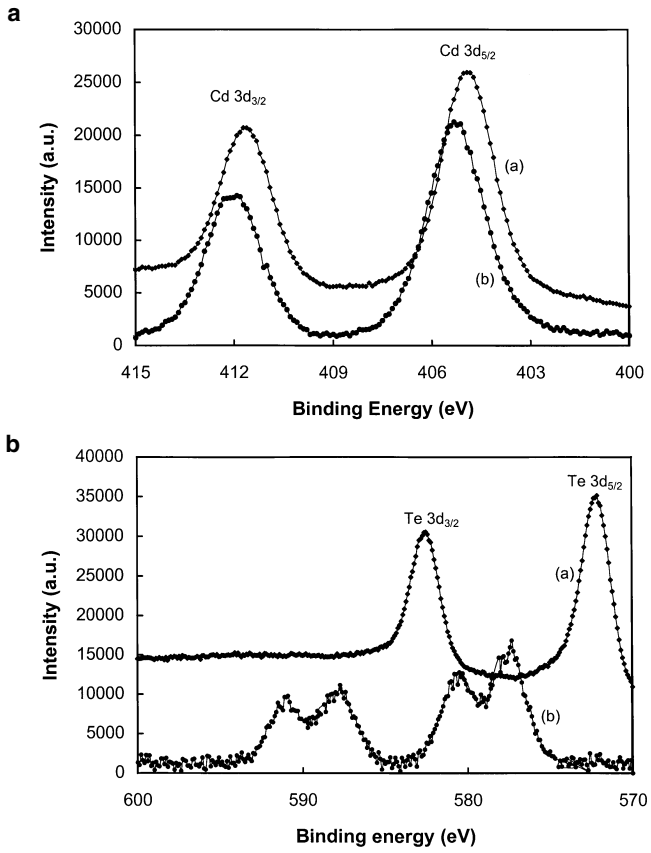

Fig. 2 XPS spectra of CdTe:TiO_2 thin film with V_f ~ 71 %, T_s = 373 K for (a) Cd $3d_{5/2}$ and Cd $3d_{3/2}$ levels; (a) as-deposited film; (b) the corresponding thermally treated film. (b) for Te $3d_{5/2}$ and Te $3d_{3/2}$ levels; (a) as-deposited film; (b) the corresponding thermally treated film.

in Fig. 1b (curves a and b), for low T_s (RT), both as-deposited and thermally treated film displays Te–O and Cd–Te related components.

Upon thermal treatment, there is a significant reduction in Te peak intensity (Fig. 1b, curve b). Here, the peak at 572.3 eV corresponds to Te in the form of CdTe, while the peak at 575.5 eV corresponds to Te oxidized to TeO_2 [5]. Similarly, for high T_s (373 K) film, upon thermal treatment, the presence of Te peak positions at 577.3 and 580.5 eV shows the formation of tellurium oxide, in particular TeO_3, and there is an appreciable reduction in Te peak intensity (Fig. 2b, curve b). The lack of Te peak at 573.5 eV corresponding to unoxidized Te [i.e., Te° for both low (RT) and high (373 K) T_s deposited films] is also a testimony to the presence of significant oxides on the surface, although the effect is felt more on the high T_s (373 K) film than on the low T_s (RT) film. The splitting of the Te $3d_{5/2}$ and Te $3d_{3/2}$ peaks indicate that Te atoms are in two different chemical environments (Te–Cd and Te–O). However, the component corresponding to the Cd–Te environment decreases drastically for thermally treated film as compared to as-deposited film (Figs. 1b and 2b, curves a and b), suggesting that CdTe bonds break upon thermal treatment. From Table 1, for as-deposited film (T_s = RT and 373 K), the low titanium concentration (~6 and 3 at % respectively) obtained is expected for TiO_2 thin films having high volume fraction (V_f ~ 50–70 %) of CdTe nanoparticles. It may also be attributed to a masking of the TiO_2 or Ti intensity by a layer of surface species that is thicker than the effective photoelectron escape depth for

the Ti 2p electrons. This effect would be more prominent after thermal treatment, and, hence, lack of any Ti XPS signal for both low (RT) and high (373 K) T_s deposited films after thermal treatment can be explained (Table 1).

As shown in Table 1, upon thermal treatment for low and high T_s (RT and 373 K) deposited films, an increase in concentration of O and substantial decrease in concentration of Te was observed. However, Cd concentration increases for both low and high T_s (RT and 373 K) films upon thermal treatment. Thus, it appears that thermal treatment has caused the breaking of CdTe bonds and possibly the depletion of free Te from the film either in the form of TeO_2 or its loss into the bulk of the film. Upon thermal treatment, Cd and Te are removed from the surface with different rates, depending upon the sublimation and evaporation properties of these two elements. Moreover, low and high T_s (RT and 373 K) films has a surface composition with Cd in excess, and this, coupled with CdTe breaking upon thermal treatment with reduction in free Te from the film, leaves the film surface rich in metallic Cd. This is further evident from the increase in Cd/Te ratio upon thermal treatment for both low and high T_s films, respectively (Table 1). This increment is mainly due to the loss of Te and increment in Cd during the thermal treatment process (Table 1).

The results for the presence of excess of Cd on the surface for thermally treated films corresponding to low and high T_s (RT and 373 K) films are in sharp contrast to the reported values where Te precipitates are usually found in CdTe crystals [7]. However, thermal treatment for both low and high T_s (RT and 373 K) films, since no splitting of the Cd 3d doublet was found, indicates that only Cd (element Cd or Cd from CdTe) is present on the surface and neither CdO nor $CdTeO_3$ is formed after thermal treatment. The presence of Te-related oxides and higher concentration of O (at %) for high T_s (373 K) films upon thermal treatment as compared to corresponding low T_s (RT) films clearly indicates that high T_s films are prone to oxidation. TeO_2 has a higher Gibbs free energy of formation (–64.6 K cal/mol) than CdO (–54.6 K cal/mol) [8]. Thus, the CdTe film exposed to the air prefers the formation of TeO_2 over CdO. As the surface tellurium is often susceptible to oxidation, it is, therefore, desirable to restrict the oxidation reaction to within a few monolayers of the surface, since TeO_2 is highly resistive [8].

Surface morphological studies

From our earlier studies [9], it has been observed that pure TiO_2 films are amorphous when grown either at RT or 373 K under conditions employed for the formation of CdTe:TiO_2 composite thin films. However, when CdTe and TiO_2 are co-sputtered under similar conditions, then CdTe nanoparticles embedded in amorphous TiO_2 matrix are formed. The SEM micrographs for thermally treated CdTe:TiO_2 composite thin films deposited at RT (300 K) and 373 K having high V_f of CdTe nanoparticles are shown in Fig. 3. As shown in Fig. 3a, for low T_s (RT) films, the microstructure precipitation of CdTe along with large-scale coalescence of Cd/CdTe islands of size ~0.3–0.7 μm is observed. Upon thermal treatment, owing to increment in metallic Cd and decrease in Te as revealed from XPS studies, the islands formed could be assigned mainly to Cd or CdTe rather than to CdO or Te. It is difficult to determine the size of the individual particles since the particles are clustered together and are highly agglomerated.

For thermally treated CdTe:TiO_2 films deposited at high T_s (373 K), since the miscibility of CdTe and TiO_2 is quite high, features of TiO_2 heavily modulated the micrograph, and it lacks the presence of distinct islands as in low T_s (RT) films but instead shows noncoalescent islands of Cd/CdTe of size ~0.15–0.3 μm (Fig. 3b). During sputtering, the TiO_2 vapor flux is substantially higher than that of CdTe, which ensures full passivation of the surface of the CdTe nanocrystals by TiO_2. Thus, increase in T_s (from RT to 373 K) increases the nucleation density of the crystals rather than the growth of already nucleated ones (Figs. 3a and 3b). However, for low T_s (RT) films, coalescence of these islands results in a continuous structure, whereas for high T_s (373 K) films, owing to the formation of a large number of isolated islands of smaller dimensions, discontinuous and disordered structure is obtained.

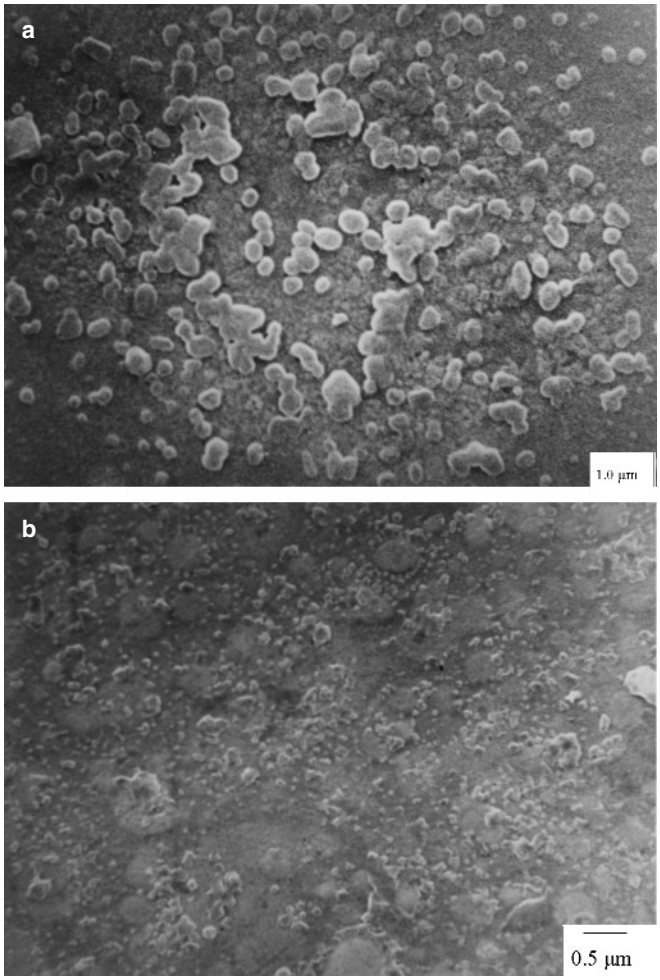

Fig. 3 SEM micrographs of nanocrystalline CdTe:TiO_2 composite films after thermal treatment. (a) for film at T_s = RT (300 K); (b) for film at T_s = 373 K.

Thus, it can be said with some certainty that the defect concentration in a film coalesced from many small islands (T_s = 373 K) is much higher than that of a film that has grown from only a few large islands (T_s = RT).

X-ray diffraction studies

From X-ray diffraction measurements, the as-deposited CdTe:TiO_2 films corresponding to T_s = RT and 373 K, are found to be mainly amorphous in nature. However, few crystalline features are realized for these films after thermal treatment. Table 2 summarizes the interplanar distance of nanocrystalline CdTe:TiO_2 films for both as-deposited and after thermal treatment. From Table 2, it is evident that interplanar distance of films deposited at high T_s (373 K) are considerably larger than the corresponding low T_s (RT) deposited films as a result of higher oxygen incorporation in high T_s films (Table 1), and this effect is felt more for films after thermal treatment. In the case of high T_s films, oxygen atoms can incorporate interstitially into the CdTe lattice, which can result in structural disorder and expansion of the interplanar distances as compared to low T_s deposited films. Since an oxygen atom has a covalent bond

Table 2 Determination of interplanar distance (nm) from X-ray diffraction data for nanocrystalline CdTe:TiO_2 films (AD: as-deposited; AT: after-thermal treatment).

System	T_s (K)	Interplanar distance (nm)	
		AD	AT
CdTe:TiO_2 (1 pellet of CdTe)	300	0.3629	0.373
CdTe:TiO_2 (3 pellets of CdTe)	300	0.3489	0.3574
CdTe:TiO_2 (1 pellet of CdTe)	373	0.3781	0.393
CdTe:TiO_2 (3 pellets of CdTe)	373	0.3703	0.3831

and ionic radii smaller than that of Cd and Te atoms, even a low oxygen incorporation within CdTe lattice could result in a strong lattice deformation.

Electrical studies

The temperature dependence of the electrical conductivity of TiO_2 films with varied V_f of CdTe nanocrystals deposited at low T_s (RT) is shown in Fig. 4a. It is observed that as the V_f is increased from 54 to 65 %, the RT conductivity of CdTe:TiO_2 films increases merely by a factor of 3.7 from 1.28×10^{-8} S cm^{-1} to 4.7×10^{-8} S cm^{-1} (Fig. 4, curve a). Similarly, for the corresponding high T_s

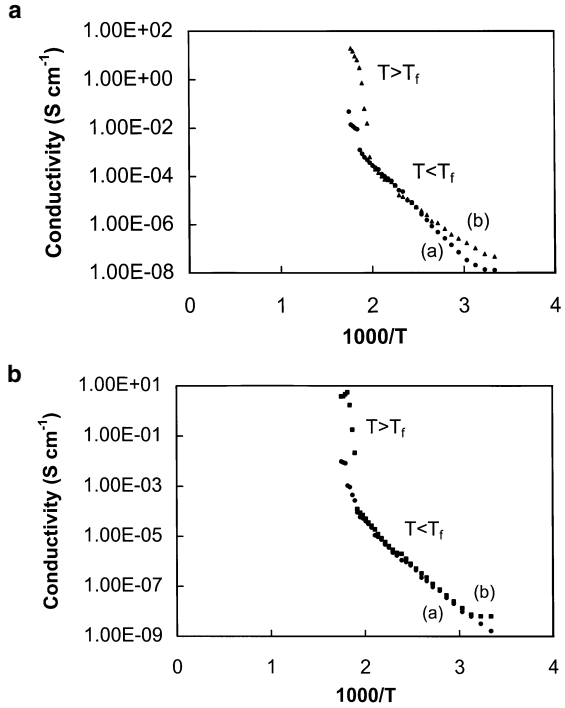

Fig. 4 Variation of dc conductivity with inverse temperature of nanocrystalline CdTe:TiO_2 composite films for (a) T_s = RT (300 K), V_f = 54 and 65 % (curves a and b); for (b) T_s = 373 K, V_f = 59 and 71 % (curves a and b).

(373 K) deposited films, increment in RT conductivity merely by a factor of ~4.0 from 1.68×10^{-9} S cm^{-1} to 6.52×10^{-9} S cm^{-1} upon increasing V_f from 59 to 71 % could be observed (Fig. 4, curve b). With the increase in V_f of semiconductor nanoparticles and decrease in intercrystallite spacing, the increase in conductivity should be expected on this basis. From Fig. 4, the conductivity is found to increase with the increase in temperature and followed the Arrehenius relation until a particular threshold temperature T_f. In the region ($T < T_f$), the dc activation energy (E_a) for the high-density films (V_f ~ 54 and 65 %) deposited at low T_s (RT) are 0.83 eV and 0.77 eV and for the corresponding films at high T_s (373 K), the E_a values are 0.81 eV and 0.72 eV, respectively. As the temperature is increased beyond T_f, the conductivity increases rapidly and irreversibly to values 4.21×10^{-1} S cm^{-1} and 3.58 S cm^{-1} corresponding to V_f ~ 54 and 65 % for low T_s (RT) deposited CdTe:TiO_2 composite thin films (Fig. 4a).

Similarly, for the corresponding films deposited at high T_s (373 K), beyond T_f, a rapid and irreversible increase in conductivity to values 1.8×10^{-2} S cm^{-1} and 2.62×10^{-1} S cm^{-1} is observed (Fig. 4b). CdTe nanocomposite films in the high conductivity state are cooled. It is found that their conductivity remains high. It is clear that these films have undergone some thermally induced change that has resulted in irreversible changes in electrical conductivity. Repeated measurement of the thermally transformed samples has yielded the same results.

Figure 5 shows the temperature dependence of the electrical conductivity of the low T_s (RT) deposited films after the transformation. As evident from Fig. 5a, these films exhibit metallic-type conduction unlike for corresponding films before thermal treatment. The conductivity of the transformed film increases with increase in V_f (54 to 65 %) with corresponding conductivity values being 4.21×10^{-1}

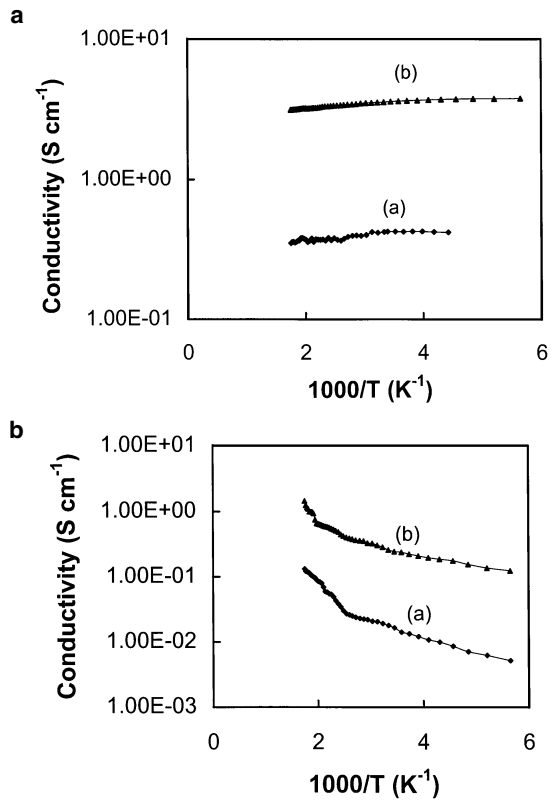

Fig. 5 Variation of dc conductivity with inverse temperature of thermally treated nanocrystalline CdTe:TiO_2 composite films for (a) T_s = RT (300 K), V_f = 54 and 65 % (curves a and b); for (b) T_s = 373 K, V_f = 59 and 71 % (curves a and b).

and 3.6 S cm^{-1} respectively (Fig. 5a, curves a and b). The activation energy for conduction of transformed films is between 4.5 and 5.0 meV, respectively. As evident from Fig. 5a, low T_s (RT) deposited films exhibited positive temperature coefficient of resistance (+ve TCR). However, for high T_s (373 K) films, the conductivity of the transformed films is found to vary exponentially with the inverse of temperature, suggesting that the conduction mechanism is thermally activated (Fig. 5b). Here, the RT conductivity values are ~1.8×10^{-2} and 2.6×10^{-1} S cm^{-1} corresponding to V_f ~ 59 and 71 %, respectively (Fig. 5b, curves a and b). These films exhibited negative temperature coefficient of resistance (–ve TCR). As these films are rich in O concentration (Table 1), small grains are surrounded by thin insulating oxide layer, which electrically insulates the grains from each other. Thus, the transfer of charge now requires activation, and this leads to negative TCR. For low T_s (RT) deposited films, thermally induced coalescence of the CdTe/Cd islands of larger size results in a connected network structure. As the inter-island distance is small, electrical conduction by percolation is favored. Moreover, segregation of metallic Cd at the surface of low T_s (RT) films as observed from XPS studies could also be responsible for metallic-type conduction exhibited by these films upon thermal treatment (Fig. 5). Our results for films with high V_f of semiconductor nanoparticles are in accordance with earlier work, where decrease in the resistivity of CdS films on annealing between 300–450 ºC was reported [10]. It was attributed to the conducting phase of CdO and Cd in the film [10]. However, in our films, the possible formation of CdO can be ruled out, and it is mainly the presence of Cd or CdTe phases that are responsible for increment in conductivity values upon thermal treatment.

The temperature T_f at which this transformation is observed is dependent on density of CdTe crystallites V_f in insulating TiO_2 matrix, and even the growth temperature affects this threshold. It is observed that T_f of films decreases with increase in V_f of the CdTe nanoparticles and films deposited at high T_s (373 K) exhibited higher transformation temperature as compared to the corresponding low T_s (RT) films. For high T_s (373 K) films, owing to the lack of formation of a proper CdTe nanocrystal network as evident from SEM studies, the transformation temperature T_f is high. However, for low T_s (RT) films upon thermal treatment, owing to coalescence of islands, the CdTe nanocrystallites form a connected network structure so that the charge carriers can percolate directly through connected CdTe or Cd grains, and it exhibits metallic behavior and, hence, low T_f.

To elucidate further the effect of the presence of the high V_f of CdTe nanocrystals on the conduction behavior of the TiO_2 thin films, σ vs. $T^{-1/2}$ studies in the temperature range of 180 K < T < 350 K were undertaken. Figure 6 shows the σ vs. $T^{-1/2}$ plot for the transformed high V_f (50–70 %) deposited

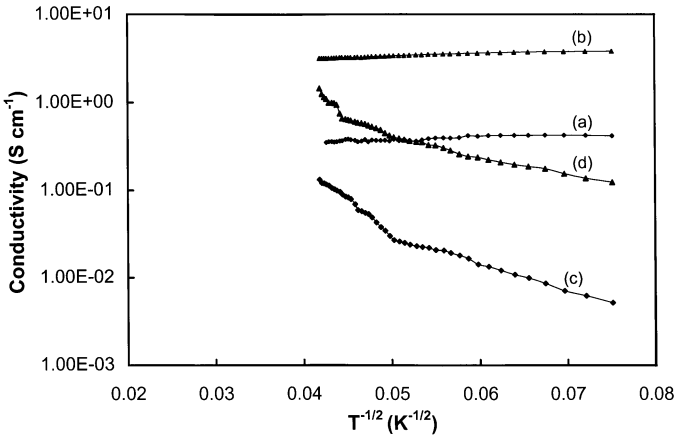

Fig. 6 Variation of dc conductivity with $T^{-1/2}$ for thermally treated nanocrystalline CdTe:TiO_2 composite films for T_s = RT (300 K), V_f = 54 and 65 % (curves a and b); and for T_s = 373 K, V_f = 59 and 71 % (curves c and d).

at low and high T_s, respectively. From Fig. 6 (curves c and d), it can be observed that the electrical conductivity decreases with decreasing temperature and exhibits a linear dependence in the σ vs. $T^{-1/2}$ plot, which is typical of a hopping transport phenomena in which charge carriers move under the influence of an applied electric field by tunneling between metal grains [11]. Here, two different slopes corresponding to high T_s (373 K) films suggests that two types of hopping mechanisms are present in these transformed films, while the electrical conductivity of the corresponding low T_s (RT) films remains essentially independent of temperature (Fig. 6, curves a and b). The slope of high T_s (373 K) films decreases with increase in V_f of CdTe nanoparticles. The conduction properties similar to the present results for the transformed high T_s (373 K) films have been commonly observed for metal-insulator composite films [12]. Here, the linear dependence of the σ vs. $T^{-1/2}$ can be interpreted as due to activated tunneling between neighboring particles, where the activation energy is taken as the electrostatic charging energy of a particle for tunneling [13]. Thus, thermally assisted tunneling between the CdTe nanocrystallites appears to be a dominant conduction process for thermally induced, transformed high T_s (373 K) films. From temperature-dependent conductivity and XPS studies, we infer that for low T_s (RT) films, electrical percolation through CdTe crystallites takes place, while for high T_s (373 K) films, electrical conduction is by hopping mechanism where charge carriers are transported from one grain to another via thermally activated tunneling.

We conjecture that for low and high T_s (RT and 373 K) films, before thermal treatment, the absence of a one-to-one relation between the excess of Cd on the surface and increment in conductivity indicates that the excess of Cd is segregated at the grain boundaries of CdTe nanoparticles until there is enough of it to make a continuous network. At this point, there is an abrupt structural change because the tendency to remain at grain surfaces is overcome by the tendency to form a bulk. It is because of this bulk behavior taking place that the low T_s (RT) films upon thermal treatment exhibits metallic-type conduction. The metallic electrical behavior of these films is due to the electrical percolation of the CdTe/Cd crystallites contained in these films. From the percolation theory, a system consisting of two phases, one more conductive than the other, will go through a percolation process at a critical concentration, which depends on the symmetry of the system. That is, at or above the critical concentration for percolation of the conductive phase, there is a sudden increase in the electrical conduction as a result of the long-range connectivity of the conductive phase [14].

In our case, for thermally treated films (T_s = RT and 373 K), the Cd concentration is always above the threshold value for the percolation to take place, however, it is mainly the substrate temperature that governs the electrical properties of the films. However, in the case of corresponding high T_s (373 K) films, even after thermal treatment, a 3D network of the crystallites could not be established owing to the formation of small and noncoalescent crystallites of Cd/CdTe. Thus, for high T_s films upon thermal treatment, even with high Cd concentration, long-range connectivity could not be realized, and, consequently, conduction mechanism was activated-type. Moreover, for high T_s (373 K) films, the surface-to-volume ratio of the crystallites is increased owing to smaller crystallites leading to a more pronounced effect of segregation than found in polycrystalline CdTe. Here, carrier loss occurs owing to trapping in states situated at the grain boundaries, which in turn define the transport properties, such as the conductivity. The mode of transport in both low and high T_s (RT and 373 K) films is different, although the conductivity increases in both with increase in the V_f of CdTe nanoparticles in the amorphous TiO_2 matrix. From the above, we can infer that it is essentially the substrate temperature, rather than metal or semiconductor concentration alone, which accounts for the changes in the transport behavior of CdTe:TiO_2 composite thin films.

CONCLUSIONS

Variations in the substrate temperature, T_s, produces two distinct structural regimes with different electrical properties in thermally treated TiO_2 thin films with high V_f of CdTe nanoparticles deposited by co-sputtering from TiO_2:CdTe target:

(a) A metallic regime, where the V_f of metal (Cd) is large and the grains touch each other and form a metallic continuum. Here, homogeneous, ordered and electrically continuous structure is obtained. Low T_f is observed owing to the presence of large-scale coalescent islands of CdTe/Cd, and, thus, 3D network of crystallites could be realized. Such films exhibit positive temperature coefficient of resistance. Electrical conduction in this regime is essentially due to electrical percolation through CdTe/Cd crystallites embedded in an amorphous matrix. XPS studies indicated the segregation of metallic Cd upon thermal treatment, which could be responsible for metallic-type conduction exhibited by these films.

(b) A nonmetallic regime in which small, isolated metal particles are dispersed in an amorphous matrix. Here, a disordered and electrically discontinuous structure is obtained. Interplanar distance of films is found to be larger owing to higher oxygen incorporation as compared to low T_s (RT) deposited films. High T_f observed here is due to the lack of formation of CdTe network. In this regime, high oxygen concentration in the form of TeO_2, etc. acts as an electrical insulation for the small and noncoalescent crystallites of CdTe/Cd. Thus, due to the formation of oxides on the surface of the grains, conduction mechanism is thermally activated. The electrical conduction in these films is essentially by hopping mechanism, indicating transfer of charge carriers via thermally activated tunneling. Such films exhibit negative temperature coefficient of resistance.

ACKNOWLEDGMENTS

We thank the Director, National Physical Laboratory for permission to publish this research work. Acknowledgments are also due to Mr. K. N. Sood of the Electron Microscopy Group for help in SEM studies.

REFERENCES

1. D. D. Beck and R. W. Siegel. *J. Mater. Res*. **7**, 2840 (1992).
2. Y. Wang and W. Mahler. *Opt. Commun*. **61**, 233 (1987).
3. B. G. Potter and J. H. Simmons. *J. Appl. Phys*. **68**, 1218 (1990).
4. Y. Suzuoki, N. Matsuno, A. Tabata, M. Takeda, T. Mizutani. *Jpn. J. Appl. Phys*. **34**, 1631 (1995).
5. A. Etchberry, F. Iranzo-Marin, E. Novakovic, R. Triboulet, C. Debiemme-Chouvy. *J. Cryst. Growth* **184/185**, 213 (1998).
6. B. J. Kowalski, B. A. Orlowski, J. Ghijsen. *Surf. Sci*. **412/413**, 544 (1998).
7. F. A. Ponce, R. Sinclair, H. Bube. *Appl. Phys. Lett*. **39**, 951 (1981).
8. X. Yi and J. J. Liou. *Solid-State Electron*. **38**, 1151 (1995).
9. A. C. Rastogi, S. N. Sharma, S. Kohli. *Semicond. Sci. Technol*. **15**, 1011 (2000).
10. S. Kolhe, S. K. Kulkarni, A. S. Nigavekar, S. K. Sharma. *Sol. Energy. Mater*. **10**, 47 (1984).
11. P. Sheng. *Phil. Mag. B* **65**, 357 (1992).
12. B. Abeles, P. Sheng, M. D. Coutts, Y. Arie. *Adv. Phys*. **24**, 407 (1975).
13. M. M. Lampart and P. Mark. In *Current Injection in Solids*, Chaps. 4 and 8, Academic, New York (1970).
14. R. Zallen. In *The Physics of Amorphous Solids*, Chaps. 4 and 6, Wiley, New York (1983).